Properties of Stationary Nonequilibrium States in the Thermostatted Periodic Lorentz Gas I: The One Particle System

F. Bonetto[†], D. Daems[‡], J.L. Lebowitz[*]

Abstact: We study numerically and analytically the properties of the stationary state of a particle moving under the influence of an electric field **E** *in a two dimensional periodic Lorentz gas with the energy kept constant by a Gaussian thermostat. Numerically the current appears to be a continuous function of* **E** *whose derivative varies very irregularly, possibly in a discontinuous manner. We argue for the non differentibility of the current as a function of* **E** *utilizing a symbolic description of the dynamics based on the discontinuities of the collision map. The decay of correlations and the behavior of the diffusion constant are also investigated.*

Keywords: Thermostatted Lorentz gas, steady state current, smoothness, regularity, symbolic dynamics.

1. Introduction

There has been much interest in modeling stationary nonequilibrium states (SNS) of physical systems by closed dynamical systems evolving under a deterministic (time-reversible) non-Hamiltonian dynamics [H][EM][GC]. This is in contrast to modeling by "open" systems with some stochastic dynamics at the boundaries or by Hamiltonian coupling to infinite reservoirs [EPR1][EPR2][BL][LS]. Some such modeling is necessary to obtain SNS since the evolution of an isolated system will only permit equilibrium stationary states (or some very unstable measures).

These dynamical system models modify the Hamiltonian time evolution by the addition of purely formal (i.e. having no connection with the actual dynamics of the system) thermostats such as a Gaussian thermostat. This keeps the kinetic or total energy of the nonequilibrium system, e.g. one subjected to external forces which do work on it and drive it away from equilibrium, constant in time thereby permitting a SNS to exist. Such a model of a stationary current carrying state produced by a steady electric field **E** acting on the charges in a conductor forming a circle (periodic boundary conditions were first introduced by Moran and Hoover [MH]). Various aspects of this model were later studied both analytically and numerically [LNRM][CELS]. It is however still not clear how well this dynamical system with its nonphysical way of extracting the heat generated by the current really models the essential features of electrical conduction in a physical system. This seems relevant to deciding on the utility of this "thermostatted" approach in nonequilibrium statistical mechanics. To answer this question we present here and in subsequent works detailed numerical and analytical studies of a class of such models describing stationary states of current carrying systems[CELS]. The system studied in the present work is the Moran-Hoover [MH] model of a single particle moving among a periodic two dimensional array of fixed scatterers (Sinai billiard) in the presence of an external field **E** and a Gaussian thermostat which keeps its kinetic energy fixed, see Fig. 1. In [BDLR],[BDGL] we consider the generalization of this model to N-particles, $N \geq 2$, see also [BGG].

The equations describing the motion of the particle, including elastic scattering with the obstacles, are:

[†] Department of Mathematics, Rutgers University, New Brunswick, NJ 08903;
Present address: IHES, 35 Route de Chartres, 91440 Bures-sur-Yvette, France, email: bonetto@ihes.fr.

[‡] Department of Mathematics, Rutgers University, New Brunswick, NJ 08903;
Present address: Center for Nonlinear Phenomena and Complex Systems, Université Libre de Bruxelles, 1050 Bruxelles, Belgium, email: ddaems@ulb.ac.be.

[*] Department of Mathematics and Physics , Rutgers University, New Brunswick, NJ 08903,
Present address: IHES, 35 Route de Chartres, 91440 Bures-sur-Yvette, France, email: lebowitz@ihes.fr.

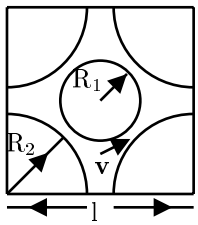

Fig. 1: General billiard structure with scatterers of radius R_1 and R_2 in a periodic box with side length l.

$$\begin{cases} \dot{\mathbf{q}} = \mathbf{v} \\ \dot{\mathbf{v}} = \mathbf{E} - \alpha(\mathbf{v})\mathbf{v} + F_{obs}(\mathbf{q}) \\ \alpha = \dfrac{(\mathbf{v}\cdot\mathbf{E})}{(\mathbf{v}\cdot\mathbf{v})} \end{cases} \tag{1.1}$$

where $(\,\cdot\,)$ represents the usual scalar product in $\mathbb{R}^2$, and we have set the mass of the particle equal to unity and $\mathbf{E} = E\hat{e}$ with $|\hat{e}| = 1$.

Eq.(1.1) and thus the full dynamics keeps the kinetic energy $\frac{\mathbf{v}^2}{2}$ fixed so that the motion takes place on the three dimensional surface of constant energy which is the direct product of a torus (with holes due to the obstacles) and the circle with $|\mathbf{v}| = v_0$. We can set $v = v_0\hat{v}$ where $\hat{v}$ is a unit vector $\hat{v} = (cos\vartheta, \sin\vartheta)$. The microcanonical or uniform distribution on this three dimensional energy surface is invariant under the dynamics when $E = 0$. For $E \neq 0$ the dynamics is not Hamiltonian. There is in fact a phase space contraction γ on the energy surface equal to $(\mathbf{E}\cdot\mathbf{v})/v_0^2$ [MH][GG][CELS].

Defining a new dimensionless time $\frac{v_0}{l}t$ where l is a characteristic length of the system (say half the length of the torus) and scaling $\mathbf{q}$ by l, $\mathbf{v}$ by v_0 and E by $\frac{l}{v_0^2}$ leave the dynamics unchanged. We shall therefore take from now on $l = 2$ and $v_0 = 1$ (we choose $l = 2$ because in this way we can see the obstacle as having centers at (0.0) and $(1,1)$). Then given any initial absolutely continuous density $\psi_0(\vartheta, \mathbf{q})$ we shall be interested in the time evolved density $\psi_t(\vartheta, \mathbf{q})$ in the limit when $t \to \infty$ which describes the stationary nonequilibrium state (SNS) of this system.

Moran and Hoover [MH] carried out extensive numerical studies of ψ_t, or more precisely of the induced measure ν_t on the Poincaré cross section parametrized by the points $P = (\alpha, \beta) \in S^1 \times [-\pi/2, \pi/2]$, α corresponding to the angle locating the point on the perimeter of the obstacle where the collision took place and β to the angle between the normal vector at α and the unit velocity vector $\hat{v}$ (see subsection 2.1 for a more precise definition). Following the discrete time trajectory P_n (in their case there was only one obstacle per unit cell of the triangular lattice, in the case of the billiard in Fig. 1 one should add an integer component to P_n, *i.e.* $P_n = (\alpha, \beta, s)$ where $s \in \{0, 1\}$ indicates which obstacle is hit) they found that the density of points for large n had a fractal appearance, *i.e.* the stationary measure appeared to be singular with respect to the uniform (microcanonical) measure $(4\pi)^{-1}\cos\alpha d\alpha d\alpha d\phi$ on P which is stationary and approached (in a weak sense) as $t \to \infty$ when $\mathbf{E} = 0$.

This problem was later studied analytically by Chernov et al. [CELS] who proved that starting with any initial density $\psi_0(\theta, \mathbf{q})$ there does indeed exist a limiting measure $\nu_t \to \nu_E^+$ for the induced measure on the Poincaré section as $t \to \infty$, whose Hausdorff dimension is, for $E \neq 0$, strictly less than two (the corresponding measure μ_E^+ on the energy surface has Hausdorff dimension less than three). They also showed that the stationary current $\mathbf{j}(\mathbf{E}) = \langle\mathbf{v}\rangle_{\mathbf{E}} = \sigma_{\mathbf{0}}\mathbf{E}[\mathbf{1} + \mathbf{o}(|\mathbf{E}|)]$ for $\mathbf{E}$ small enough $|\mathbf{E}| < E_0$, $E_0 << 1$ (possibly as small as 10^{-20}) where $\langle\cdot\rangle_E$ is the average with respect to μ_E^+ and σ_0 (generally a tensor) is given by the Kubo formula. (It also follows from their analysis that $\mathbf{j}(\mathbf{E})$ is continuous for $|\mathbf{E}| < E_0$.)

In the present work we examine $\mathbf{j}(\mathbf{E})$ and other properties of the stationary measure ν^+ for $E \in (0.025, 2)$ and $\hat{e} = \hat{x}$,*i.e.* the field is in the x direction and so $\mathbf{j}(\mathbf{E}) = j(E)\hat{x}$. Carrying out a numerical evaluation of the Kubo formula for σ_0 (*i.e.* an integral of the autocorrelation function at zero field) we find good agreement with the results of the simulation for $j(E)$ as E tends towards zero. A similar investigation, with less precision for small values of E, was carried out for a triangular geometry in [LNRM], where the results, which look similar to ours for E not too small, were analyzed in terms of periodic orbits. Here we focus on the behavior of the current for $E \in (0.025, 0.5)$ where rather precise numerical simulations indicate nonsmooth behavior of $j(E)$ vs. E. In particular we analyze the apparent singularities of ν_E^+ as a function of E in terms of the change in the

singularities of the map from P_n to P_{n+1} caused by grazing collisions as E changes. We also analyze the formal expression for the derivatives of $j(E)$ obtained from the Kawasaki formula [CELS], and the equivalent Ruelle formalism [R]. We identify possible origins of singularities and argue for a function $j(E)$ that is non differentiable or, at most, admits a weak derivative with a dense set of discontinuities although the non rigorous nature of our argument does not permit a definitive statement (a similar statement should hold for the dependence of $\mathbf{j}(\mathbf{E})$ on $\hat{e}$).

It should be noted that, as shown in [ER] the stationary current is directly related to the sum of the stable and unstable Lyapunov exponents of the system via the equality $(\mathbf{j}(\mathbf{E})\cdot\mathbf{E}) = -[\lambda^s(\mathbf{E}) + \lambda^u(\mathbf{E})]$. There is also a relation between the Hausdorff dimension of μ^+ and the Lyapunov exponents $D_H(\nu^+) = 1 - \lambda^u(\mathbf{E})/\lambda^s(\mathbf{E})$ (remember that $\lambda^s(0) + \lambda^u(0) = 0$ but $\lambda^s(\mathbf{E}) + \lambda^u(\mathbf{E}) < 0$ for $E \neq 0$).

In addition to $\mathbf{j}(\mathbf{E})$ we also investigate the diffusion constant $d(E)$ relative to the drift as a function of E and compare it to $d\mathbf{j}(E)/dE$, equality constituting in the limit $E \to 0$ the Einstein relation proven in [CELS]. Finally we compute the decay of the velocity autocorrelation function for $E \neq 0$ and analyze the numerical results using the methods developed in [GG]. We find that the decay continues to be exponential (this was proven for $E = 0$ in [Y]) with an oscillatory behavior which changes qualitatively at or close to those values of E at which we see the nonsmooth behavior in the higher derivatives of $\mathbf{j}(\mathbf{E})$.

2. Current versus field: results and discussion

We first describe the results of our simulations and then discuss possible theoretical explanations of their most interesting features.

2.1. Numerical results

We used three different methods to compute the current as a function of the field for the model in Fig. 1 with $R_1 = 0.39$, $R_2 = 0.79$[1] and $|\mathbf{v}| = 1$. The first two are based on the fact that the system appears to be ergodic for $E \lesssim 2$ (this has been proved only for the case when the field is very small, see [CELS]). This allows us to compute the current by choosing a "typical" initial point and evolving it for a very long time while measuring the time average of the instantaneous current.

The simulations were done by computing a trajectory of 10^9 successive collisions. The only difficulty in the algorithm is in computing the successive collision times in a fast enough manner without missing collisions that are nearly tangent. Our algorithm is based on a Newton method: it takes around 20 hours to compute 10^9 successive collisions on a i586 processor with a 350 Mhz clock under a Linux operating system. The values of $\kappa(E) = j(E)/E$ obtained by the simulation are represented by the filled points in Fig. 2. The error-bars are computed by running 10 independent initial conditions and looking at the maximum and minimum values obtained in this way. It is reasonable to believe that, while the value of the current averaged over a long time T goes to 0 as the field goes to 0, the fluctuations about that average with respect to the initial point should be more or less independent of E. Considering the heavy numerical work needed to evolve 10 points for 10^9 successive collisions we did it for $E = 0.025$, 0.05, 0.1, 0.125 and 0.175 and interpolated linearly for the error-bar at other points (the reason of the choice to leave out only $E = 0.75$, 0.150 and 0.2 is because we think nothing new happens there in a sense that will become clear in the following subsection).

To obtain more confidence in our numerics we also computed $\kappa(E)$ using the Kawasaki formula which allows us to compute also $\kappa(0)$ (for a rigorous proof of this formula when E is very small see [CELS]). Letting $S_E(t, X)$, with $X = (\mathbf{q}, \mathbf{v})$, be the evolution generated by (1.1) and calling $J(X)$ the velocity component along the direction of $\mathbf{E}$, then $j(E) = \langle J(X)\rangle_E$ with $\langle\cdot\rangle_E$ representing the average with respect to μ_E^+, one has the Kawasaki formula[CELS],

$$\kappa(E) = \int_0^\infty dt \langle J(X) J(S_E(t, X))\rangle_0 \tag{2.1}$$

where $\langle\cdot\rangle_0$ represents the average with respect to the microcanonical distribution corresponding to μ_0^+. Observe

[1] These values coincide with the one used in [BGG]. There a system with many particles was studied and the radia were set to $R_1 = 0.4$, $R_2 = 0.8$ plus a particles' radius of $r = 0.01$. It is clear that if only one particle is present this is equivalent to a point particle moving among scatterers with radii $R_1 = 0.39$ and $R_2 = 0.79$.

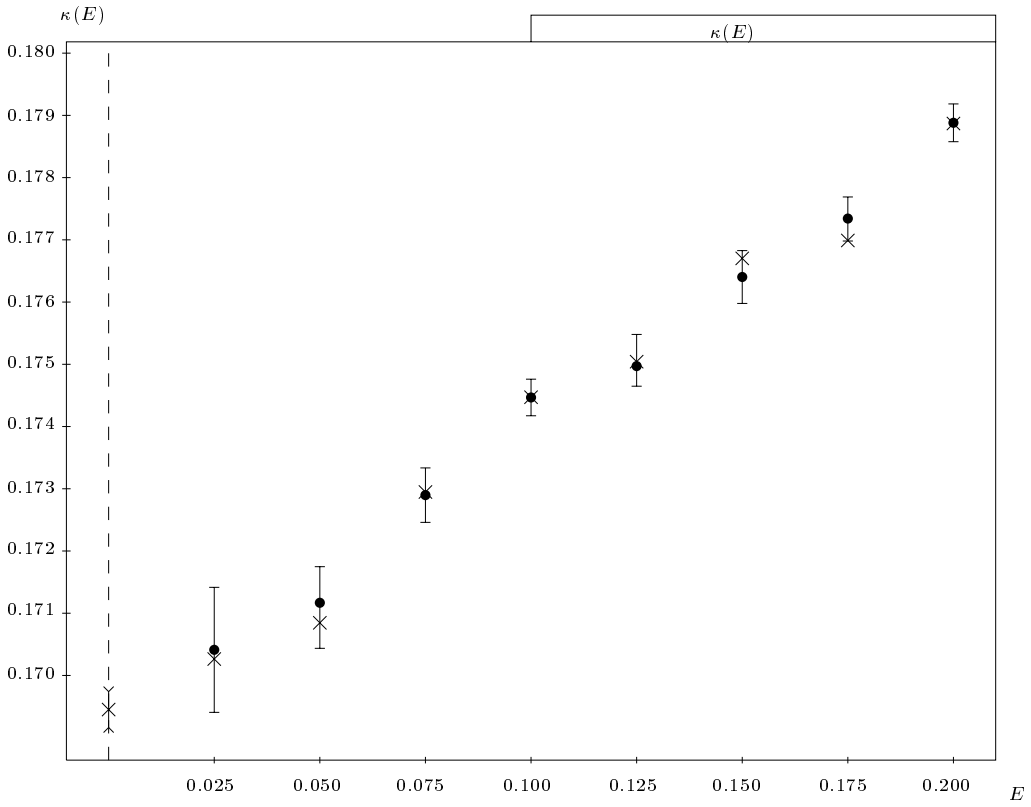

Fig. 2: Conductivity as a function of the field E. The filled circles represent the results from the time average on a single long trajectory with their error-bar. The crosses represent the result from the Kawasaki simulation. No error-bar is reported in this case (except for the value at $E = 0$) to enhance readability. In any case the errors on the Kawasaki values are larger than the ones on the long time averages.

that eq.(2.1) reduces for $E = 0$ to the well known Green-Kubo expression for the linear response to an external field.

There are two problems in using eq.(2.1) numerically. The first is the necessity of a very good random number generator for the initial conditions and the second is the impossibility of integrating the correlation function for long times if one wants to have good statistics. We solved the first problem by using a R250 generator (see [NR]) and, to ensure a better independence, we decorrelated the initial points by evolving then for 40 collisions without field. In this situation we observed that at a time equal to 50 times the mean free flight time the correlation function in eq.(2.1) is of the order of 10^{-4} allowing us to say that the truncation error is probably much smaller than the statistical error due to the fact that we evolved only $2 \cdot 10^6$ initial conditions. Observe that in this case we can assume that our experiment consists in the independent sampling of a random variable so that we can estimate the statistical error by its variance divided by the square root of the number of initial points. We observe finally that this method, although numerically demanding, is theoretically more reliable than the first method used to get the filled points in Fig. 2 due to the intrinsic instability of the dynamics under consideration, see [GG] for a more precise discussion.

The results of this simulation are also plotted in Fig. 2 using crosses. We report the error bar only for the value at $E = 0$ to maintain readability of the graphs. We note that the error-bars for $E > 0$ are approximatively twice that at $E = 0$ (simulations at $E = 0$ are much easier and faster). This means that all the values are in within the error bar of those computed with the previous method.

Due to the symmetry of our system we clearly have that $\kappa(E) = \kappa(-E)$ so, assuming that $\kappa(E)$ is a smooth function of E we should be able to fit it for small E by $\kappa(E) = \kappa(0) + \kappa''(0)E^2$. Such a fit is indeed possible (in particular one would find $\kappa(0) = 0.169$ and $\kappa''(0) = 0.53$) but it will pass only through the error-bars of the first three points. From the fourth point on the graph has a very linear appearance (to be precise we can fit it well by $\kappa(E) = 0.169 + 0.042E$). The problem with this linear fit is that it would produce a discontinuity of the first derivative of $\kappa(E)$ at some value of $E \in (0.05, 0.075)$. Moreover, due to the very large error-bars near $E = 0$, it is easy to see that the linear fit for $E > 0.075$ passes through the error-bars of all the points leaving

open the possibility of a discontinuity of the first derivative of $j(E)$ at $E = 0$.

Clearly the question of discontinuities in the derivatives cannot be decided on the basis of numerical simulations. We need an analytical argument (to be transformed hopefully into a proof) to decide this question. We present such an argument in the following subsection. But we first show in Fig. 3 a graph of the current for higher value of the field to see if other discontinuities of the derivative can be seen. We used the first method described before Fig. 2 to compute the current from $E = 0.2$ to $E = 2.0$ at steps of $\Delta E = 0.025$. Each run consisted of $5 \cdot 10^7$ collisions and the error bars have been computed for values of $E = 0.25 + 0.25i$ by running 10 initial condition and interpolated for the other points (when they are not visible it is because they are smaller than the points).

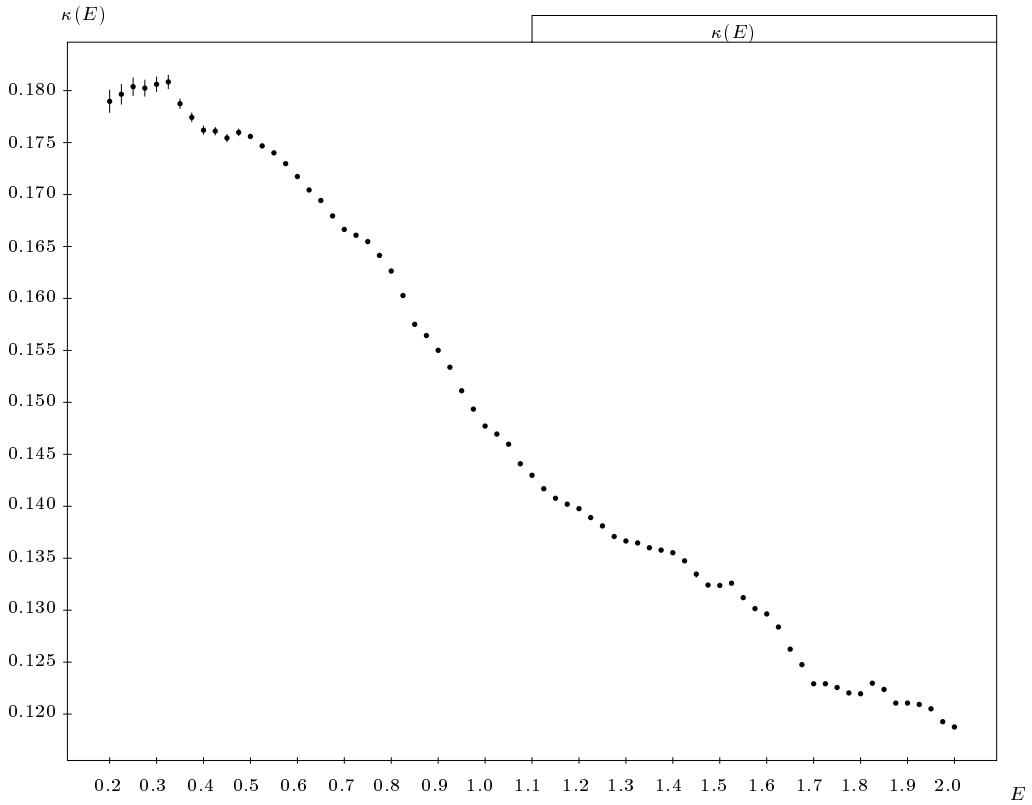

Fig. 3: Behavior of the current for higher value of the field. When no error-bar is visible it means that it is smaller than the symbol used.

Based on Fig. 3 it seems consistent to assume that $\kappa(E)$ is continuous for $E < 2$. Its derivative on the contrary continues to change in a very irregular, possibly discontinuous, way. The first value of E at which a big change is seen is around $E = 0.35$. To better appreciate this we plot the conductivity for $E = 0.2$ to $E = 0.5$ in Fig. 4.

As can be easily seen the most probable site of discontinuous behavior of the derivative are at fields in the intervals $(0.225, 0.25)$, $(0.325, 0.35)$ and $(0.375, 0.425)$. After discussing the possible origin of non smooth behavior of the expectation of a smooth function with respect to μ_E^+ we will return to the behavior of $j(E)$ at those values of E.

We briefly report on a third method to compute the value of the conductivity that we used to be sure that the above results are not due to a bias in our Newton scheme. The idea is the same as the first method but instead of the fast Newton style algorithm we used a discrete time integrator (a fourth order Runge-Kutta integrator). To avoid missing collisions that are almost tangent we had to choose a very small time step, *i.e.* $\delta t = 10^{-4}$. The slowness of this algorithm permitted us to check only a few points and they were consistent with the other methods.

We close this section observing that our simulations support the validity of a central limit theorem for our system. In fact if one looks at the behavior of the maximum and minimum values observed among the ten

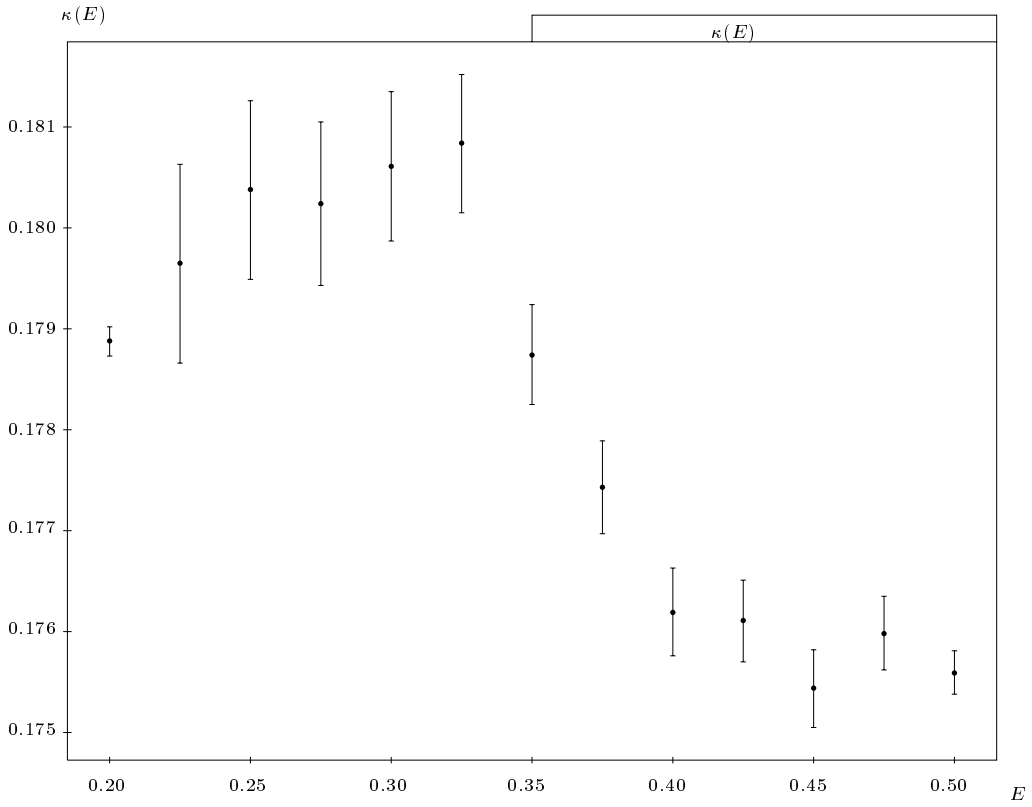

Fig. 4: Current versus field for $E \in [0.2, 0.5]$. The intervals $(0.225, 0.25)$ and $(0.325, 0.35)$ and $(0.375, 0.425)$ possibly contain discountinuity of the first derivative.

runs as a function of the running time T one finds that one can fit it with a function of the form $C/\sqrt{T}$ with $C \simeq \langle J(X)^2\rangle_E - \langle J(X)\rangle_E^2$.

2.2. Analytical discussion

To study the properties of $\kappa(E)$ as a function of E we can use eq.(2.1). We know that the correlation functions in eq.(2.1) are uniformly integrable for $E < E_0$ for some very small E_0, see [CELS]. This allows us to exchange limits,

$$\begin{aligned}\lim_{E\to E'} \int_0^\infty dt \langle J(X) J(S_E(t,X))\rangle_0 = \\ \int_0^\infty dt \langle J(X) \lim_{E\to E'} J(S_E(t,X))\rangle_0 = \\ \int_0^\infty dt \langle J(X) J(S_{E'}(t,X))\rangle_0\end{aligned} \tag{2.2}$$

and conclude that $\kappa(E)$ is a continuous function of E for $E < E_0$. Although the argument in [CELS] gives, as already stated, a very small value for E_0 the numerical results, some of which are reported at the end of this subsection, support the validity of the above reasoning at least for $E \lesssim 1$.

Differentiating eq.(2.1) to obtain the higher derivatives of $\kappa(E)$ as a function of E is essentially equivalent to what is formally done in [R]. We obtain

$$\frac{d\kappa(E)}{dE} = \int_0^\infty dt \int_0^t dt' \langle J(X) F(S_E(t',X)) \cdot \nabla_{S_E(t,X)} J(S_E(t-t', S_E(t',X)))\rangle_0. \tag{2.3}$$

where $F(X) = \hat{x} - (\hat{x}\cdot \mathbf{v})\mathbf{v}$ is the derivative respect to E of the right hand side of eq.(1.1). This can be rewritten as:

$$\frac{d\kappa(E)}{dE} = \int_0^\infty dt \int_0^t dt' \langle J(X) J(S_E(t',X)) J(S_E(t,X))) \rangle_0 + \int_0^\infty dt \int_0^t dt' \langle \nabla_{S_E(t,X)} J(X) \cdot F(S_E(t',X)) J(S_E(t,X))) \rangle_0 \tag{2.4}$$

Observe that the second term on the right hand side can be rewritten as:

$$\int_0^\infty dt \int_0^t dt' \langle \nabla_X J(X) \Lambda^{-1}(t',X) F(S_E(t',X)) J(S_E(t,X))) \rangle_0 = \int_0^\infty dt \int_0^t dt' \langle \hat{x} \Lambda^{-1}(t',X) \hat{x} J(S_E(t,X))) \rangle_0 + \int_0^\infty dt \int_0^t dt' \langle \hat{x} \Lambda^{-1}(t',X) \cdot \mathbf{v} J(S_E(t',X)) J(S_E(t,X)) \rangle_0 \tag{2.5}$$

where $\Lambda(t,X)$ is the tangent flow generated by $S(t,X)$, *i.e.* $\Lambda(t,X) = \frac{\partial S(t,X)}{\partial X}$. Eq. (2.4), together with analogous expressions for the higher order derivatives can be obtained easily from the formalism developed in [R]. Note that since the system has Lyapunov exponents $\lambda^u(E) > 0$ and one $\lambda^s(E) < 0$ (at least for not too large E) one should expect that $\hat{x}\Lambda^{-1}(t',X)\hat{x} \simeq e^{-\lambda^s(E)t}$. This makes the convergence of the integrals in (2.5) very problematic. We will return to these equations later after we consider this question from a different point of view[2].

It is convenient at this point to introduce a discrete time version of our dynamical system making precise what was already sketched in the introduction. For every point X in phase space we can define $\tau(X)$ as the first time at which the particle collides with one of the scatterers. Let now $\mathcal{S}_E(X) = S_E(\tau(X)^+, X)$ where the $^+$ indicates that we choose the velocity after the collision. It is clear that $\mathcal{S}_E(X)$ restricted to the set $\mathcal{T}$ of points $X = (\mathbf{q}, \mathbf{v})$, such that $\mathbf{q}$ is on the surface of an obstacle and $\mathbf{v}$ is directed outward of the obstacle, defines a dynamical system (the set $\mathcal{T}$ is usually called a Poincaré section). We can parametrize the collision points P in $\mathcal{T}$ by two angles and an integer, *i.e.* (α, β, s) where $s \in \{0,1\}$ is 0 if the point is on the obstacle with radius 0.79 and 1 if it is on the obstacle of radius 0.39, $\alpha \in [-\pi, \pi]$ is the angle between the direction of the field and the point on the scatterer at which the particle collides and $\beta \in [-\pi/2, \pi/2]$ is the angle between the outgoing velocity and the normal direction to the scatterer, see Fig. 1. We can also write $\mathcal{T} = \mathcal{T}^0 \cup \mathcal{T}^1$ where $P \in \mathcal{T}^s$ iff $P = (\alpha, \beta, s)$. With a slight abuse of notation we will still indicate our dynamical system in the new coordinates by $\mathcal{S}_E(P)$ (note that for $E = 0$ the invariant measure on $\mathcal{T}$ is proportional to $sin\beta d\beta d\alpha$).

As we already mentioned in the introduction the invariant measure μ_E^+ for $S_E(t,X)$ will induce a measure ν_E^+ for $\mathcal{S}(P)$ on $\mathcal{T}$. The average of any function $G(X)$ with respect to μ_E^+ can be obtained from ν_E^+ via:

$$\langle G(X) \rangle_E = \frac{1}{\tau_E^+} \int_{\mathcal{T}} \mathcal{G}(P) d\nu_E^+(P) \tag{2.6}$$

where $\mathcal{G}(X) = \int_0^{\tau(X)} G(S_E(t,X)) dt$ and $\tau_E^+ = \int_{\mathcal{T}} \tau(P) d\nu_E^+(P)$.

A very useful tool for the discussion of regularity properties of dynamical system in terms of external parameters consists in the construction of a conjugating map, *i.e.* we can look for a family of functions $h_{E,E'}(P)$ with the property that:

$$\mathcal{S}_E(h_{E,E'}(P)) = h_{E,E'}(\mathcal{S}_{E'}(P)). \tag{2.7}$$

see [BKL] for an example of such a construction for an Anosov systems. It is easy to see that for smooth dynamical systems (*e.g.* Anosov or axiom A) such a family exists, at least in a small neighborhood of any given E, and the average of a smooth function has the same regularity properties as the conjugation[JLl][BKL]. In our case the existence of a smooth family $h_{E,E'}$ of conjugation would not be enough to prove that if $\mathcal{G}(P)$ is a smooth function then $\langle \mathcal{G} \rangle_E^d = \int_{\mathcal{T}} \mathcal{G}(P) d\nu_E^+(P)$ is a smooth function of E. One would also have to show that the local unstable foliation as a function of E has good smoothness property[3]Ẇe will not touch this second point

[2] Much of the following material is the result of discussions that the authors had with G. Gallavotti, N. Chernov, L.-S. Young, D. Ruelle and C. Dettman. We are particularly indebted to G. Gallavotti for explaining to us a possible method to construct a Markov partition for the billiard, construction that forms the basis of our analysis of the conjugation map.

[3] See [BKL] for a precise discussion of this point.

and focus our attention on the conjugation, hoping that an answer to the problem of its existence will give us enough information on the smoothness of the $\kappa(E)$.

The main problem with our system is that the map $\mathcal{S}_E(X)$ is only piecewise smooth[4]. In fact $\mathcal{S}_E(X)$ is smooth except at points whose image is tangent at collision[5], *i.e.* the discontinuity set $\mathcal{E}_E^1$ of $\mathcal{S}_E(P)$ is defined by the set of P such that $\mathcal{S}_E(P) = (\alpha', \pm\pi/2, s)$ for some α'. It is clear that we can divide $\mathcal{E}_E^1$ into two parts $\mathcal{E}_E^{1,s} = \mathcal{E}_E^1 \cap \mathcal{T}^s$ corresponding to the two obstacles. Moreover, due to the time reversibility of the dynamics it is easy to see that if $(\alpha, \beta, s) \in \mathcal{E}_E^1$ then $(\alpha, -\beta, s)$ is in the discontinuity set $\mathcal{E}_E^{-1}$ of $\mathcal{S}_E^{-1}$. The set $\mathcal{E}_0^{1,1}$ is shown in Fig. 5.

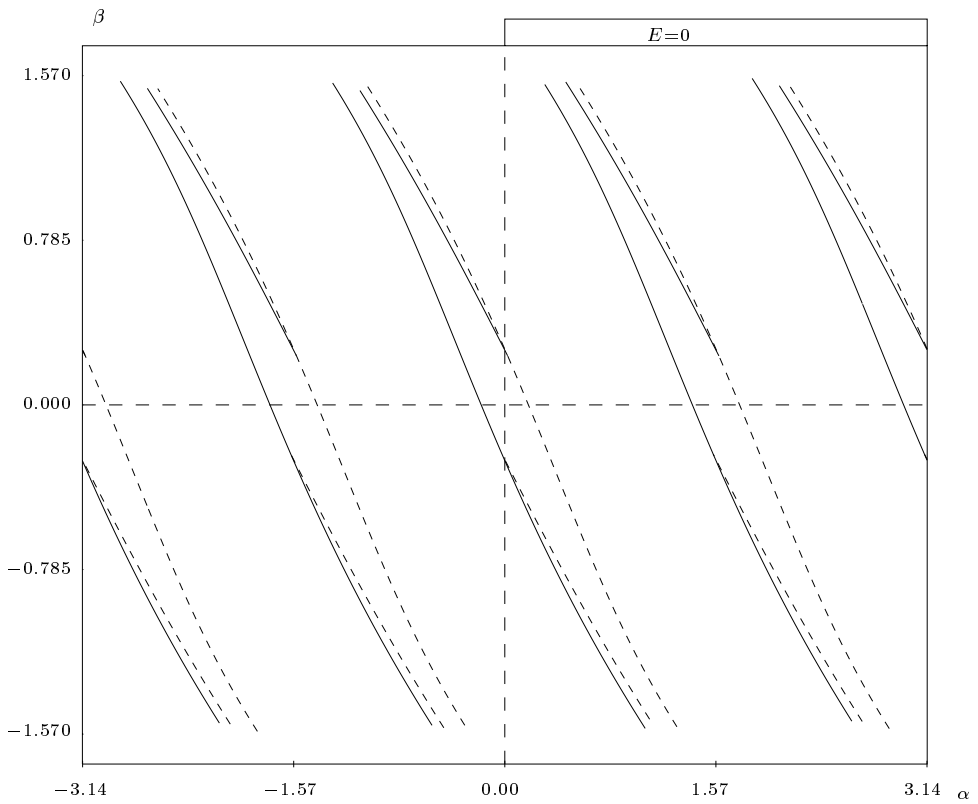

Fig. 5: Discontinuity set $\mathcal{E}_0^{1,1}$ for the map $\mathcal{S}_0$ on the obstacle of radius 0.39: the solid lines represent points that collide with $\beta = \pi/2$ while the dashed lines represent points that collide with $\beta = -\pi/2$. The α has to be thought of as periodic.

This set is formed by a finite number of disjoint locally one dimensional manifolds with possibly a finite number of bifurcations (see Fig. 5). The bifurcation points are the points P where a multiple tangency happens, *i.e.* where the β-component of both $\mathcal{S}_E(P)$ and $\mathcal{S}_E^2(P)$ is in $\{-\pi/2, \pi/2\}$. It is also easy to see that the boundary points of these manifolds are in $\beta = \pi/2$ or $\beta = -\pi/2$ and that every branch of $\mathcal{E}_E^1$ can be represented by an increasing function $\alpha(\beta)$. Although Fig. 5 has been generated with the help of the molecular dynamics program described in the previous section it would not be difficult to write analytical expressions for the manifolds in $\mathcal{E}_E^1$. We note that from eq.(2.6) we get that $\langle J(X)\rangle_E = \langle \mathcal{J}(P)\rangle_E^d / \tau_E^+$ where $\mathcal{J}(P)$ is not a smooth function on $\mathcal{T}$. This should not be a problem considering that $\mathcal{J}$, as any function $\mathcal{G}(P)$ obtained from a smooth function $G(X)$ on phase space in the same way, is discontinuous exaclty on $\mathcal{E}_E^1$ and smooth everywhere else.

It is also easy to observe that $\mathcal{I}_E^1 = \mathcal{E}_E^{-1} \cap \mathcal{E}_E^1$ is a discrete set with a finite number I_E of points P_i. We can assume that I_E is a piecewise constant function of E and one can write $P_i = P_i(E)$ for every $P_i \in \mathcal{I}_E^1$ with $P_i(E)$ defined and smooth on every open interval on which I_E is constant. Moreover the points $P_i(E)$, together with the bifurcation points, divide the manifolds to which they belong into connected segments and these segments

[4] We will use the term smooth in the vague sense of "sufficiently differentiable": at the level of rigor of the forthcoming discussion it is not worthwhile to specify exactly what kind of regularity we need. This ambiguity should not undermine the understandability of the following reasoning.

[5] The trajectories issuing from these points are usually called "grazing trajectories"

form the sides of polygons (generically squares and triangles at this level) that form a partition of $\mathcal{T}$. Again we can assume that, for E in a small enough interval, these segments and polygons can be smoothly parametrized. Fig. 6 presents a snapshot of this situation for $E = 0$.

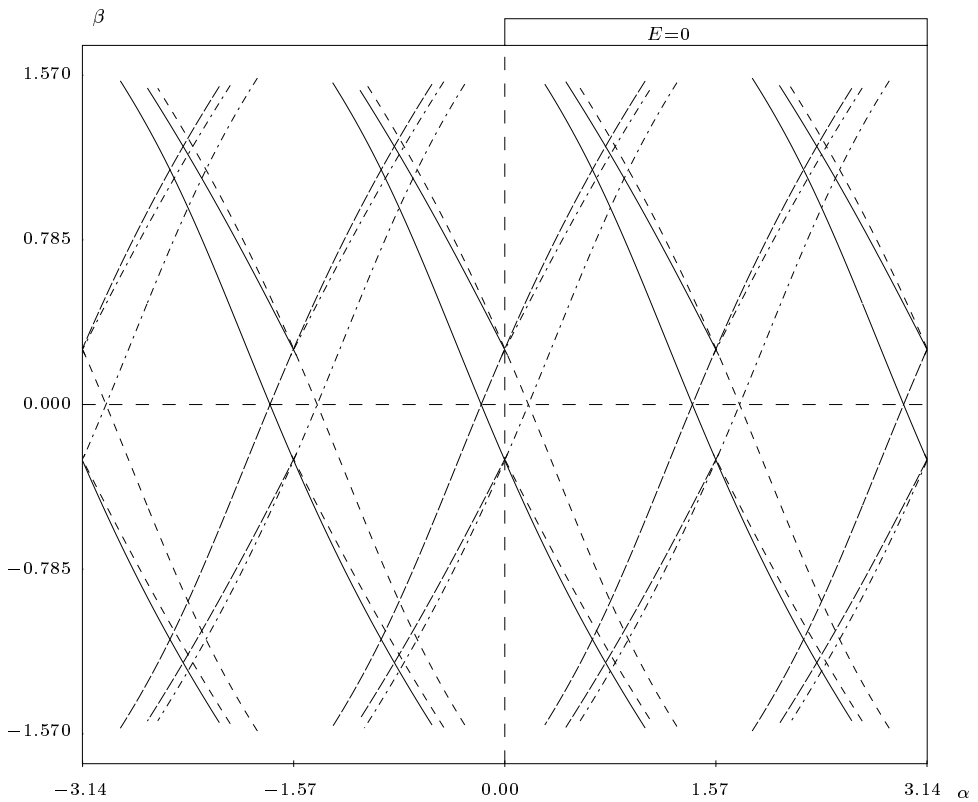

Fig. 6: Discontinuity set $\mathcal{E}_0^{1,1}$ and $\mathcal{E}_0^{-1,1}$ for the map $\mathcal{S}_E(P)$ on the obstacle of radius 0.39

It is clear that any conjugating map $h_{E,E'}$ has to map $\mathcal{E}_E^1$ to $\mathcal{E}_{E'}^1$ and $\mathcal{E}_{E'}^{-1}$ to $\mathcal{E}_{E'}^{-1}$. A possible first approximation of such an $h_{E,E'}$ consists in defining $h_{E,E'}^{(1)}(P_i(E))\big|_{\mathcal{I}_E^1} = P_i(E')$. It is clear that such a map can be extended to a smooth map $h_{E,E'}^{(1)} : \mathcal{T} \to \mathcal{T}$ such that $h_{E,E'}^{(1)}(P) = P + (E' - E)\delta h_{E,E'}^{(1)}(P)$ where $\delta h_{E,E'}^{(1)}$ is some smooth function and $h_{E,E'}^{(1)}(\mathcal{E}_E^\sigma) = \mathcal{E}_{E'}^\sigma$ for $\sigma = \pm 1$.

Although the map $h_{E,E'}^{(1)}$ is surely not a conjugation we can consider it as a starting point and reproduce the above construction using the sets of discontinuities of $\mathcal{S}_E^2(P)$ and of $\mathcal{S}_E^{-2}(P)$, $\mathcal{E}_E^2$ and $\mathcal{E}_E^{-2}$ respectively, obtaining a new map $h_{E,E'}^{(2)}$. Observe that $\mathcal{E}_E^2 = \mathcal{E}_E^1 \cup \tilde{\mathcal{E}}_E^2$ where $P \in \tilde{\mathcal{E}}_E^2$ iff the β-component of $\mathcal{S}_E^2(P)$ is in $\{-\pi/2, \pi/2\}$. An example of the set $\tilde{\mathcal{E}}_E^2 \cup \tilde{\mathcal{E}}_E^{-2}$ is given in Fig. 7

It is well known that the sets $\mathcal{E}_E^N$ will become dense as $N \to \infty$ so one can hope that the above construction will create a sequence of functions $h_{E,E'}^{(N)}$ eventually converging to a real conjugation when $N \to \infty$. Moreover, considering that all the so constructed approximations are smooth one can hope that also the limit will be smooth. There is nevertheless a major problem that makes such a convergence impossible, at least in this first naive meaning, as we will see in what follows.

Let us again consider our first approximation $h_{E,E'}^{(1)}$. It is easy to realize that we can associate to each of the connected regions in which $\mathcal{E}_E^{1,s}$ divides $\mathcal{T}^s$ a pair of integer $\mathbf{c} = (n_x, n_y)$ indicating the difference in coordinates between the center of the obstacle with which the particle collides and the one from which it starts. From now on we will see the dynamics as taking place on the universal covering of the torus and we will assume that the origin coincides with the center of one of the scatterers of radius 0.79. We will denote the set of this pair of integers by $\tilde{D}_E^{1,s}$ and call it the set of possible "forward histories of lenght one" for reasons that will become clear in what follows. Observe that the map $\mathcal{S}_E$ is continuous from one side at every point on $\mathcal{E}_E^1$. This

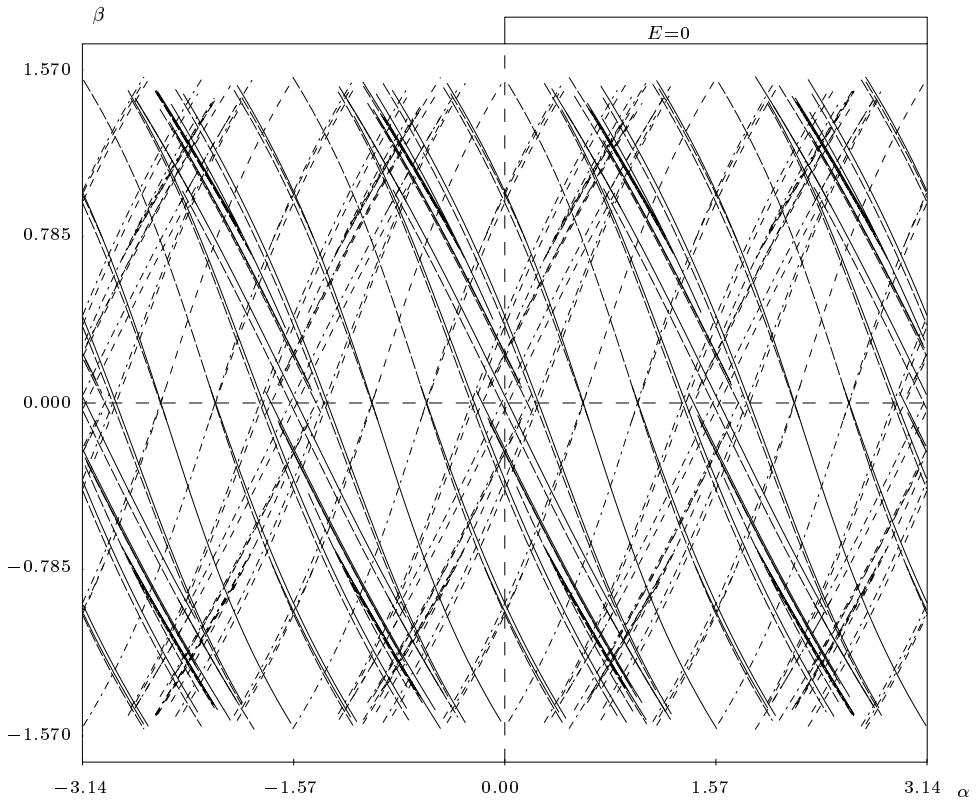

Fig. 7: Discontinuity set $\mathcal{E}_0^{2,1}$ and $\mathcal{E}_0^{-2,1}$ for the map $\mathcal{S}_E(P)$ on the obstacle of radius 0.395

allows us to define the set $D_E^{1,s} \subset \tilde{D}_E^{1,s}$ of the pair of integers associated with points in $\mathcal{E}_E^{1,s}$ (these represent the obstacles that can be grazed starting from a given obstacle). In Fig. 8 we show, in the two upper pictures, the set $D_E^{1,1}$ for $E = 0$ and $E = 0.45$. One can realize that two new obstacles can be grazed at a field $E = 0.45$ whereas they were not at a field $E = 0$. The two lower pictures show the corresponding appearence of a new branch of $\mathcal{E}_E^1$ and the fact that a new connected component of $\mathcal{T}^1 \backslash \mathcal{E}_E^1$ is created. The number on the figures are meant to help associate corresponding regions. The real modification of the set $D_E^{1,1}$ takes place at some value of $E \in (0.375, 0.4)$ but we show the situation at $E = 0.45$ because it would otherwise be difficult to observe it due to the small size of the region denoted by 5 in the lower right picture in Fig. 8. It is interesting to note that this change takes place in one of the intervals where we located a possible discontinuity of the derivative of $\kappa(E)$. We believe that this phenomenon is at the origin of those discontinuities and we will argue in this sense in what follows.

Let us call E_d the exact value of E at which the new possible histories appear. We can still construct our map $h^{(1)}_{E_d-\delta E, E_d+\delta E}$, for a very small δE, mapping the regions numbered from 1 to 4 in Fig. 5 for $E = E_d - \delta E$ in to the corresponding ones for $E = E_d + \delta E$. This would create the first approximation $h^{(1)}_{E_d-\delta E, E_d+\delta E}$ to what we can call a "partial conjugation" $h_{E_d-\delta E, E_d+\delta E}$ to be obtained as a limit of functions $h^{(N)}_{E_d-\delta E, E_d+\delta E}$ constructed iterating the above scheme. Using this function to compute the average of a smooth function on $\mathcal{T}$ as a function of E would give a smooth result but we will commit an error due to the missed region corresponding to the new possible history (region 5 in Fig. 5). It is easy to realize that this region will have a size proportional to $\sqrt{\delta E}$ and thus an area proportional to δE. We can assume, as a first approximation, that the error committed in neglecting such a region is proportional to this area which would give a discontinuity in the first derivative.

We will now check if we can use this idea to account for the other points of discontinuity we have indicated in the previous section. First of all we observe that something very similar to what we discussed above happens in the interval $(0.325, 0.35)$ with the role of $D_E^{1,1}$ played by $D_E^{1,0}$, as shown in Fig. 9.

Although it seems to agree quite well with the numerical observations this picture is still very partial. In fact it can happen that the set $\mathcal{I}_E^1 = \mathcal{E}_E^{-1} \cap \mathcal{E}_E^1$ changes structure although the sets $\mathcal{E}_E^{\pm 1}$ remain structurally identical.

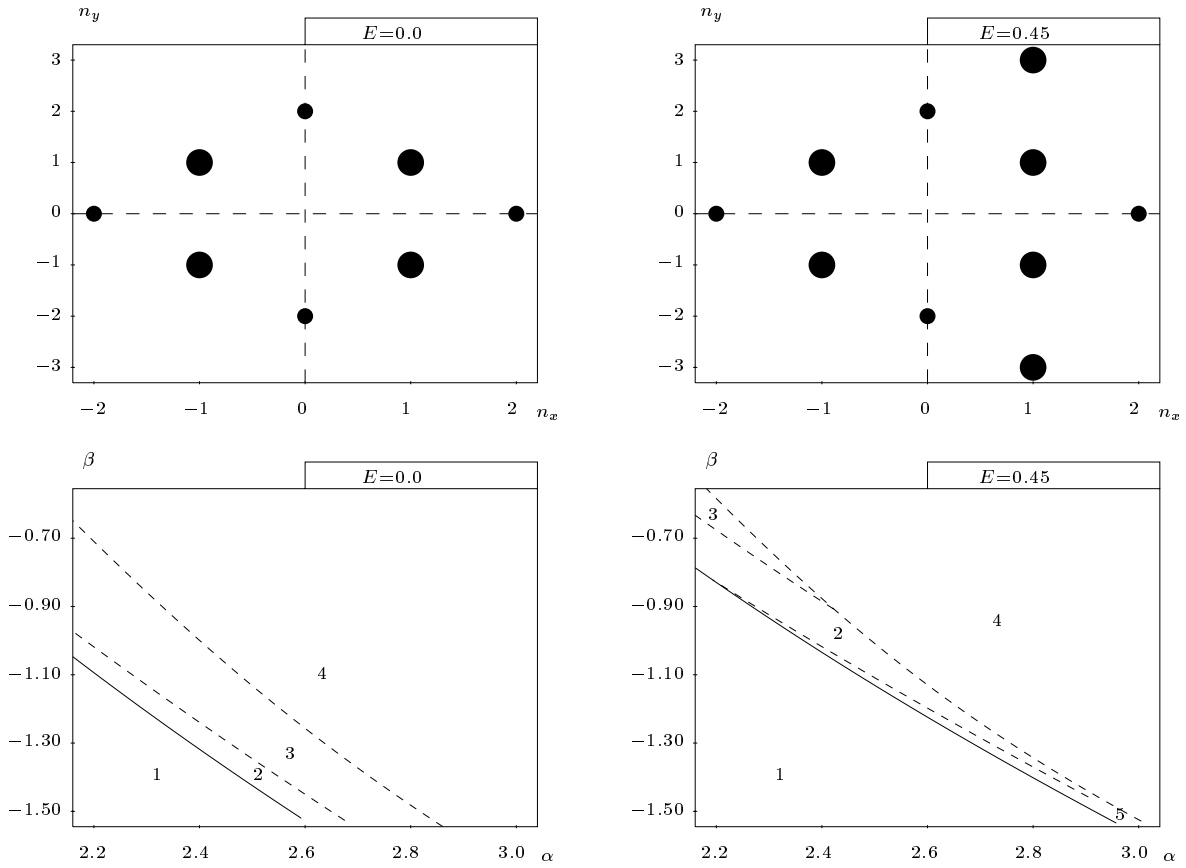

Fig. 8: $D_E^{1,1}$ for $E = 0$ and $E = 0.45$ with a detailed wiev of a part of the corresponding set $\mathcal{E}_E^{1,1}$ showing the appearence of a new branch and a new connected component in $\mathcal{T}^1 \backslash \mathcal{E}_E 1, 1$ (numbers represent corresponding regions). Although the sizes are not to scale a larger point stands for an obstacle of radius R_2.

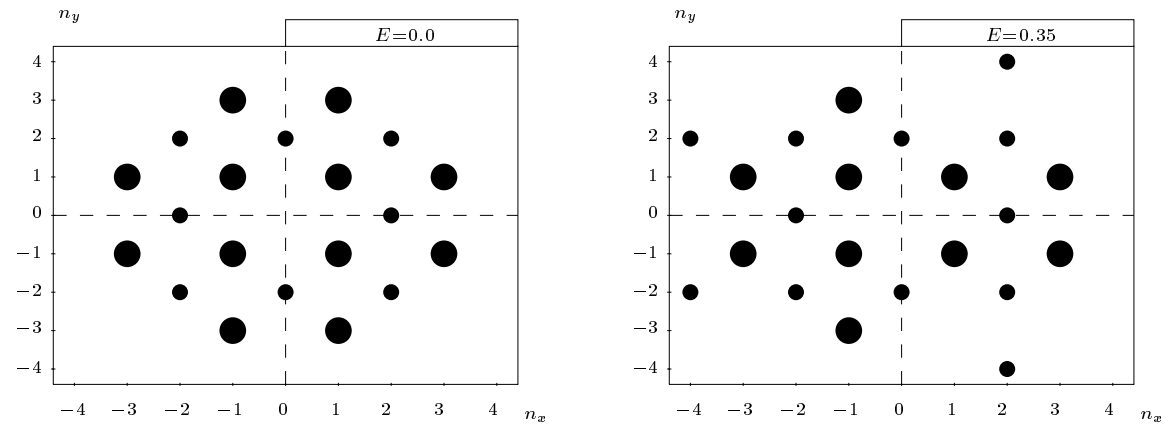

Fig. 9: $D_E^{0,1}$ for $E = 0$ and $E = 0.35$.

It is possible to see from Fig. 6 that almost all the points in $\mathcal{I}_E^1$ are near bifurcation points for $\mathcal{E}_E^{\pm 1}$. Looking carefully at the picture (see Fig. 9) one realizes that there are indeed 4 intesection points that delimit a small square. We observe that, as we did before, we can associate with every polygon in $\mathcal{T}$ bounded by $\mathcal{E}_E^{-1,s} \cup \mathcal{E}_E^{1,s}$ a

sequence of length 2 $(\mathbf{c}_{-1}, \mathbf{c}_1)$ of pairs of integers $\mathbf{c}_i = (n_{x,i}, n_{y,i})$ representing the center on which the particle collides forward and backward in time. We can call the set of all these pairs the possible "symmetric history of length two" and denote it by M_E^1. If one follows the evolution of the above mentioned square as a function of the field one realizes that at a field in $(0.05, 0.075)$ it disappears (see Fig. 9). We can again reason as before to deduce that this phenomenon will give rise to a discontinuity of the first derivative. The possible definition of the map $h^{(1)}_{E,E'}$ in this situation appears more complex and we will not discuss it here leaving this question and a formalization of the above picture to a forthcoming study.

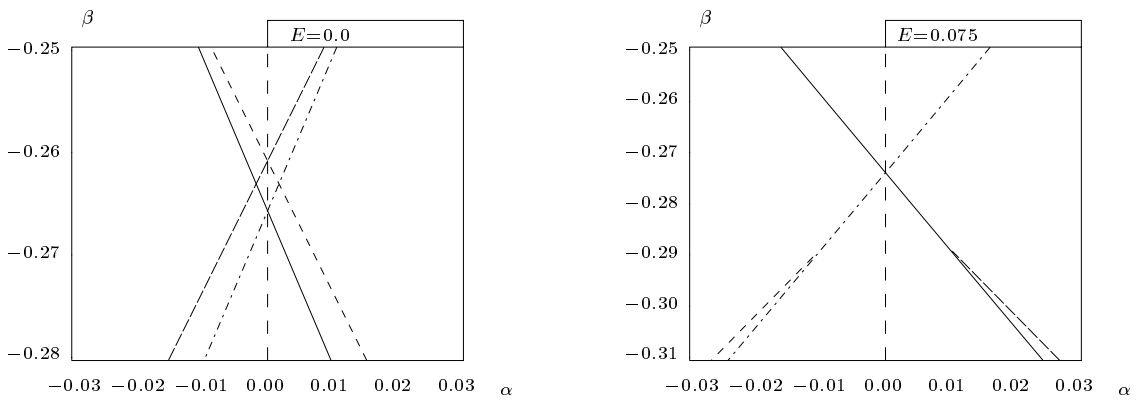

Fig. 10: Detail of $\mathcal{E}_E^{1,1} \cup \mathcal{E}_E^{-1,1}$ showing the change of I_E^1 although $\mathcal{E}_E^{s,1}$ changes smoothly

We observe here that the above considerations can be iterated. We can consider the set $D_E^{N,s}$ formed by sequences of length N, $(\mathbf{c}_1, \ldots, \mathbf{c}_N)$ of pairs of integers representing the possible consecutive collisions that a trajectory experiences starting from the obstacle s (we can call it the set of possible "forward histories of length N"). With a reasoning analogous to the one above we can expect a discontinuity of the first derivative when one of this set changes. It is easy to see that, as N grows, the number of histories in the set D_E^N increases exponentially and, due to the instability of the dynamics, new possible histories will appear or disappear very often. On the other hand each of the regions in which $\mathcal{T}$ is divided by the set $\mathcal{E}_E^N$ is exponentially small in N so we can expect them to create exponentially small discontinuities of the first derivative. A similar argument holds for the set $\mathcal{I}_E^N$ and the set of symmetric histories of length $2N$. This suggests that one should be able to define a "partial conjugation between E and E'" mapping $\mathcal{T} \backslash \Sigma_{E,E'}$ to $\mathcal{T} \backslash \Sigma_{E',E}$ where $\Sigma_{E',E}$ and $\Sigma_{E,E'}$ are two sets with area proportional to $|E' - E|$ and a very complex structure, possibly fractal. Considering our comments after eq.(2.7) this would suggests that $\kappa(E)$, as well as the average of any other smooth function on phase space, is never differentiable or that its derivative exists only in a weak sense and has a dense set of discontinuities.

We note here that in the interval $(0.25, 0.275)$ several of the above phenomena take place (*i.e.* D_E^2 and D_E^3 change and a symmetric history of length two disappears) so that a precise discussion of what happens is not possible at this point.

The above picture may seem unnatural and without hope of rigorous formalization and practical use. In this respect it is interesting to note that one can consider the polygons that are rectangles in Fig. 6 as part of a Markov partition[6]. Indeed not all of them will have the necessary property of covariance but it is possible to give a theoretically simple algorithm to detect which can be considered as part of a Markov partition. The part of phase space not covered by these squares should be analyzed using the discontinuity set of $\mathcal{S}_E^2$. This will permit to obtain more squares and to cover a bigger portion of phase space. Clearly this algorithm can be iterated and, hopefully, will give rise to a complete Markov partition. In this situation our partial conjugation map is obtained by simply matching points with the same symbolic history. Although the above description seems quite vague we think that the algorithm can be explicitly written and implemented on a computer. We hope to come back to this point in a forthcoming work.

[6] We use this notion in a weaker sense than the usual meaning of a partition of $\mathcal{T}$, in a possibly denumerable set of rectangles whose boundaries are mapped covariantly one to the other.

We conclude this section with two remarks:

- One is typically used to think of conjugation as mapping the unstable manifold of one system into the unstable manifold of the other and similarly for the stable. Our proposed map, in some sense really does this. In fact the set $\mathcal{E}_E^N$ will get more and more parallel to the unstable local foliation of our system. An analogous comment holds for the Markov partition.

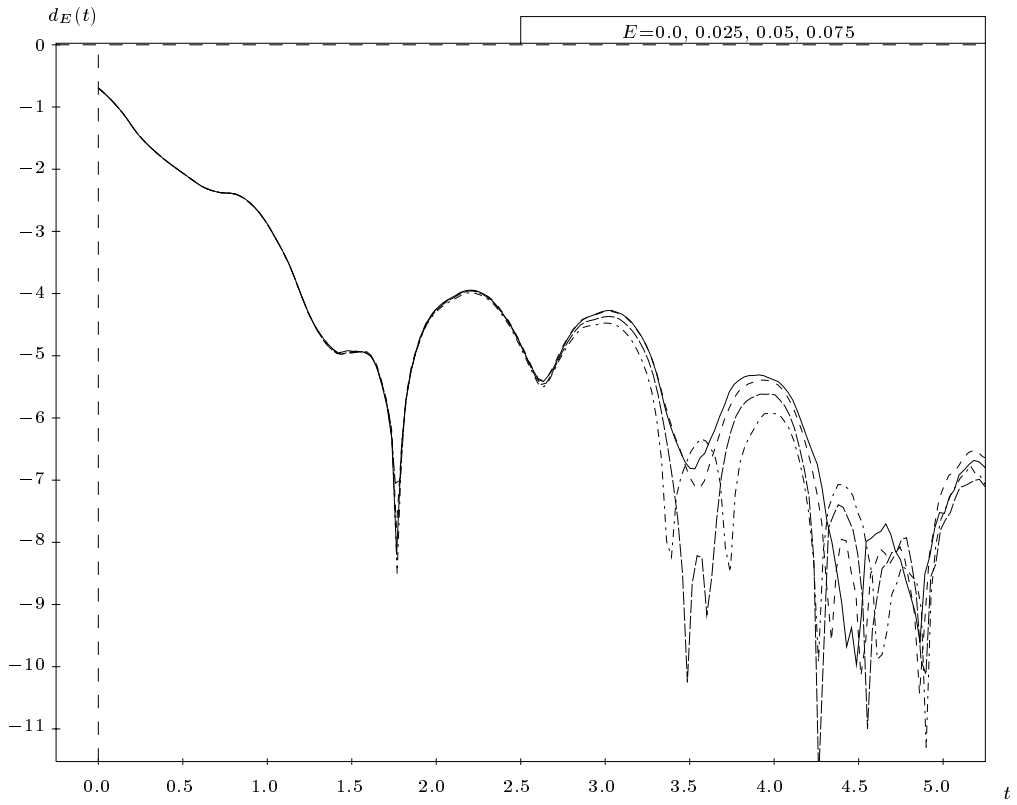

Fig. 11: Logarithm of orrelation function with respect to the the Lebesgue measure for fields $E = 0$ (solid line), $E = 0.025$ (short dashed), $E = 0.05$ (long dashed) and $E = 0.075$ (dotted dashed).

- An idea of this situation can come also from (2.5). Indeed it is reasonable to think that $\Lambda_E(t, X)$ will be given by a function that is smooth everywhere except on the discontinuity generated by the collisions that happen before time t. This implies that if X is part of a grazing trajectory for a given E_0 we can expect $\Lambda_E(t, X)$ to be non smooth as a function of E at $E = E_0$. Considering that the set of grazing trajectories varies smootly with E and that (2.5) contains an integral over the variable X we do not expect any non-smoothness of the current to take place before the set of grazing trajectories changes its structure. A dimensional analysis gives the same result as for the conjugation but we do not report it here because we do not believe that the integrals in (2.5) converge. We show instead in Fig. 11 the behavior of $d_E(t) = \log(|D_E(t)|)$ with $D_E(t) = \langle J(X)J(S_E(t, X))\rangle_E$ as a function of t and E. We see that all these functions have a maxima for t near 3 and near 4. The value at the maximum is a decreasing function of the field. In general the correlation function appears to be decreasing in E at fixed X except for the appearence of a new maximum around $t = 3.5$. We think that this new maximum can be connected with the appearence of a new symbol in D_E^3 and so with the discontinuity in the derivative of $\kappa(E)$ for small E. We leave this point as a speculation because checking it is beyond the scope of this paper.

3. Correlation function and diffusion coefficient

In addition to $D_E(t)$ we studied the current-current correlation function in the steady state:

$$C_E(t) = \langle J(X)J(S_E(t,X))\rangle_E - \langle J(X)\rangle_E^2$$

To compute this function we used a method similar to the one used for computing the Kawasaki formula. After having generated an initial point using the R250 generator we evolve it for 20 collisions with the field $E = 0$ to better decorrelate the initial choice. We then switch on the field and let the system evolve for 50 collisions in such a way that the final point can be considered as distributed according to the stationary SRB distribution μ_E^+. We then use such a point to compute a trajectory segment of lenght 40 over wich we compute the correlation. For small values of the field the correlation function $C_E(t)$ appears very similar to the Kawasaki correlation function. Considering that we already plotted $C_0(t) = D_0(t)$ in Fig. 13 we plot the logarithm of the correlation function $c_E(t) = \log(|C_E(t)|)$ for $E = 0.025$, 0.05, 0.075 and 0.1.

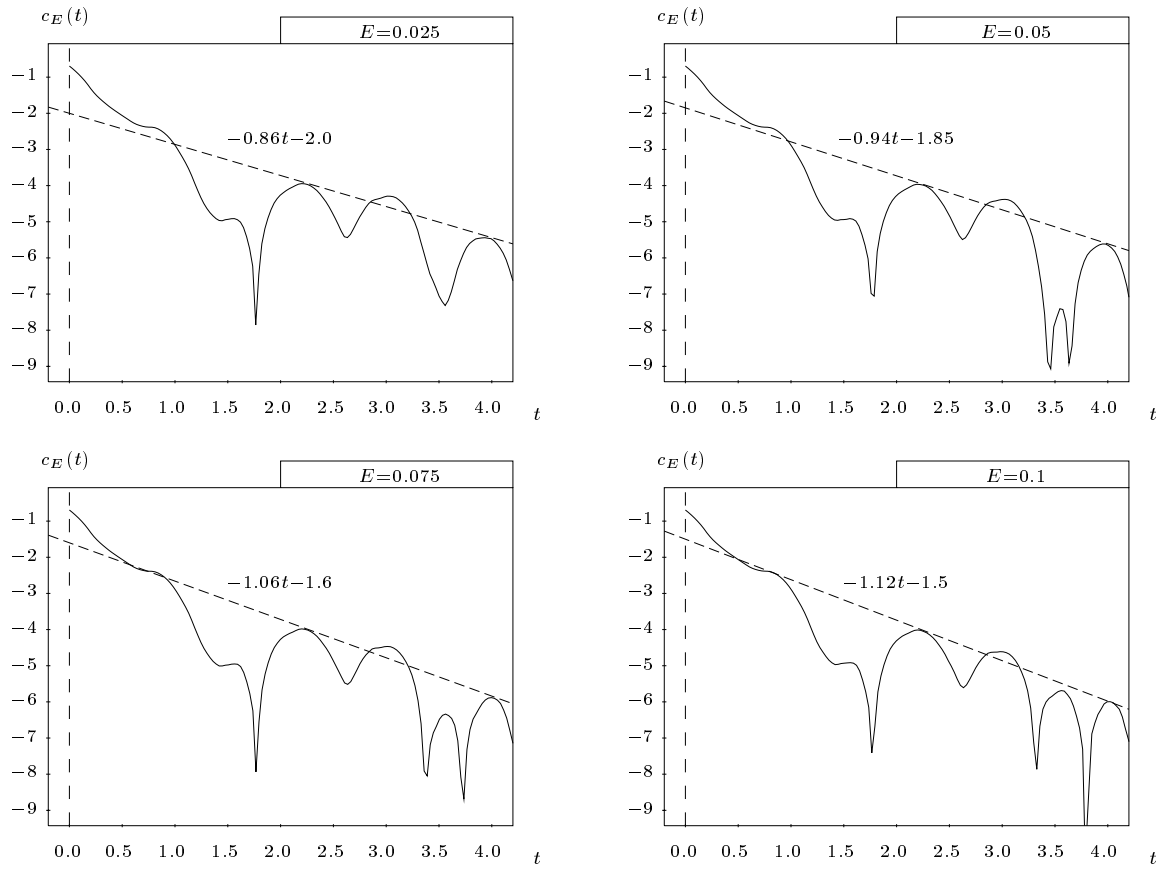

Fig. 12: Estimation of the decay of the correlation function for $E = 0.025$, 0.05, 0.075 and 0.1 using a linear fit for the maxima of $c_E(t)$

One of the most interesting question about such correlation functions is whether it decay exponentially. In the case $E = 0$ it has been proven in [Y] and the proof can be extended for small (possibly very small) value of the field [C]. We use here a method developed in [GG] to analyze this question. In that paper the exponential decay rate was obtained by dividing the set of maxima of the function $c_0(t)$ into two groups and fitting them by a linear law. Due to the fact that our simulations are shorter than the one used in [GG] (mainly for the reason that computing the collision time for $E \neq 0$ is much harder than for $E = 0$ since the exact solution contains transcendental functions) we see two maxima only for one of the two groups used in [GG]: the maximum near $t = 2$ and the one near $t = 4$. While a fit for $E = 0$ gives us a value consistent with the one obtained by [GG][7]it is evident that the slope of the fitting line becomes more negative (*i.e.* a faster exponential decay) when the field is switched on. A numerical value can be deduced from the fit reported in Fig. 12 but we do not plot them separately because the error bar on each point would be too large.

[7] Note that our results are reported in our adimensional time while in [GG] they were reported in unit of the mean free fly time

As already noted before the structure of $c_E(t)$ changes as E changes. Moreover it seems to us (although with our data we cannot really make a definitive statement) that one would still be able to divide the maxima of the correlation function into groups each of which well fitted by a linear law whose slope depends on E[8]. This behavior can be explained if one assumes that the correlation function is given by a sum of (quasi)-periodic functions modulated by decaying exponentials. Such a behavior is well established in the case of a diamond billiard by the numerical work in [ACG]. The hypothesis formulated at the end of the previous section will mean, in this setting, that the terms in the above sum are linked with the symbolic dynamics of the system. We hope to come back to this problem in a forthcoming work.

We computed the correlation function $C_E(t)$ also for values of the field in the interval $(0.275, 0.4)$. All the above discussion can be applied to this case in the same way and we do not show any graphs because no new information can be obtained from them. The integral of the correlation function $C_E(t)$ gives us the xx-element of the diffusion matrix for the system, *i.e.* $d(E) = \int_0^\infty C_E(t)dt$. We conclude this paper reporting the value of this quantity obtained from the above data.

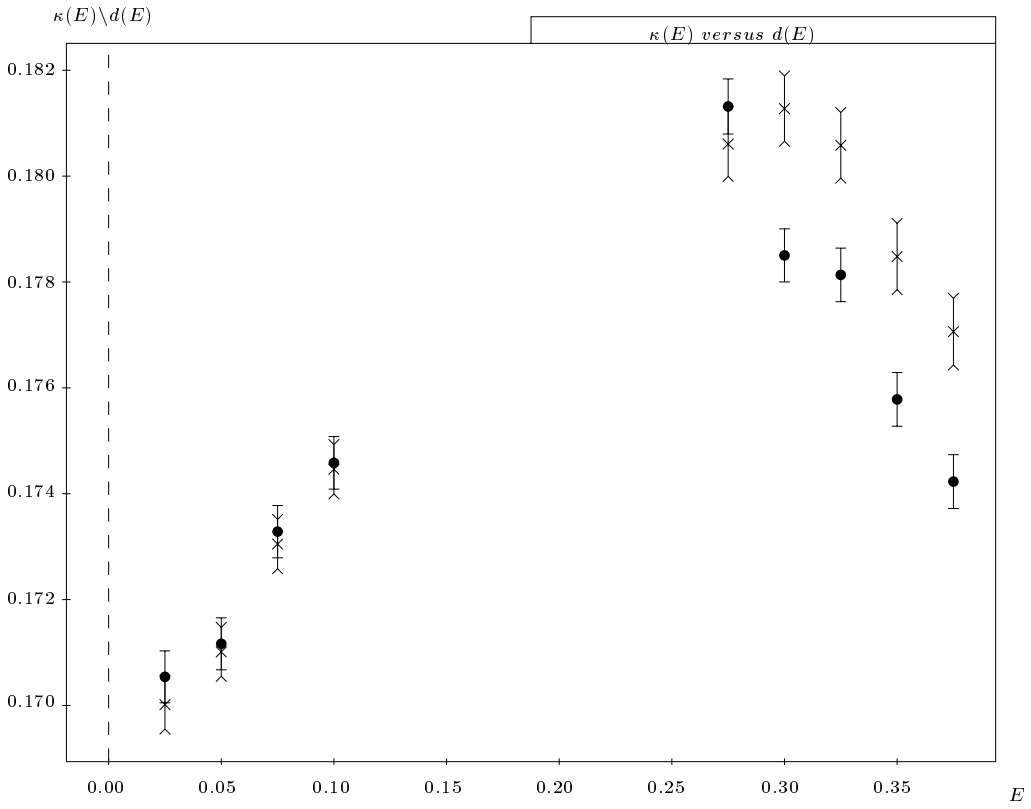

Fig. 13: $d(E)$ versus $\kappa(E)$ showing good agreement near $E = 0$ but clear non equality at $E \neq 0$

As for the correlation function we have the data for $E \in (0.025, 0.1)$ and $E \in (0.275, 0.375)$. In Fig. 13 the value of the diffusion coefficient is plotted together with the value of $\kappa(E)$ obtained from the Kawasaki formula. It is clear that for small fields the two formulas give almost the same value. Such an equality for $E \neq 0$ would support the possibility of the validity of a Green-Kubo relation out of equilibrium[GG][ES]. Our results show that the Kawasaki formula and the Green-Kubo relation give different results for $E \neq 0$.

4. Conclusions

In this paper we presented results of numerical simulations as well as analytical evidence for a non smooth

[8] In [GG] all the two groups of maxima where fitted by linear laws with the same slope. It is unclear whether such a property can be expected when $E \neq 0$

behavior of the current as a function of the field in a thermostatted single particle model of electrical conduction. We mainly studied the invariant measure ν_E^+ for the discrete time dynamical system obtained by considering as timing events the collisions of the particle with the obstacles. Our analysis is based on (at the present nonrigorous) construction of a conjugation map or rather a "partial conjugation map" between the dynamics at two different values of the field E. This construction strongly relies on the expectation that it is possible to analyze the dynamics using symbols directly connected to the discontinuities of the collision map. The picture can probably be substantiated by constructing in a explicit way a Markov partition for the dynamical system.

Our analysis implies that the average with respect to ν_E^+ of any smooth function on $\mathcal{T}$ or, more generally, the average of every smooth function on phase space with respect to μ_E^+ is a not twice differentiable with respect to the electric field E. Moreover one can conjecture that the first derivative exists in a weak sense but is everywhere discontinuous. Such a behavior has already been observed in [KD] for a very simple model.

While our analysis is not rigorous it has the advantage of being, at least in principle, contructive. The scheme for the construction of a "partial conjugation" or better of a Markov partition can lead to a rigorous proof of our assertions together with the possibility of conducting computer assisted experiments on the billiards.

As noted earlier the recent formalism developed by Ruelle in [R] suggests the presence of the same kind of non smoothness but we do not see a possibility of using it in a convincing way to argue in one direction or the other. It seems to us that a form of conjugation would be in any case necessary to show the convergence of eq.(2.3).

We also analyze the behavior of the velocity-velocity correlation function and of the diffusion coefficient. Applying the methods developed in [GG] we argue that the correlation functions decay exponentially also when the field is non zero. Moreover the rate of decay appears to increase with the field, at least for small values of E. The detailed structure of the correlation function undergoes interesting changes and we try to correlate these changes with the property of the invariant measure discussed above. Due to the numerical difficulties of computing correlation functions our discussion remains speculative.

Finally we computed the diffusion coefficient. For $E = 0$ the diffusion coefficient gives the linear conductivity. It has been argued that this relation could be valid also for a field different from 0, see [ES]. This would imply that the integral of the correlation function computed with respect to the Lebesgue measure, $d_E(t)$, and with respect to the SRB measure μ_E^+, should be equal. Our results show that this is not the case so that no direct extention of a Green-Kubo formula to non-equilibrium is possible (see [G] for an interesting proposal of what exending Green-Kubo out of equilibrium means). Results similar to ours were already present in [ES]. Considering that no good reason has ever been given for the above equality to hold we consider this result as natural.

Acknowledgment We are greatly indebted to G. Gallavotti, N. Chernov, L.-S. Young, D. Ruelle and C. Dettman for many enlightening discussion. Research supported in part by NSF Grant DMR-9813268. D.D. aknowledges support from the Francqui Foundation. We aknowledge support and ospitatlity from the IHES where this work was finished.

References.

[ACG] R. Artuso, G. Casati, I. Guarneri: Geometric scaling of correlation decay in chaotic billiards, *Phys. Rev. E* **51** (1995) R3807-R3810

[BDGL] F. Bonetto, D. Daems, J.L. Lebowitz, V. Ricci: Properties of Stationary Nonequilibrium States in the Thermostatted Periodic Lorentz Gas II: The many point particles system, in preparation

[BDLR] F. Bonetto, D. Daems, P.L. Garrido, J.L. Lebowitz: Properties of Stationary Nonequilibrium States in the Thermostatted Periodic Lorentz Gas III: The many colliding particles system, in preparation

[BGG] F. Bonetto, G. Gallavotti, P.L. Garrido: Chaotic Hypothesis: an experimental test *Physica D* **105** (1997), 226-252

[BKL] F. Bonetto, A. Kupiainen, J.L. Lebowitz: Perturbation theory for coupled Arnold cat maps: absolute continuity of marginal distribution, in preparation

[BL] P.G. Bergaman, J.L. Lebowitz: *Phys. Rev.* **99** (1955) 2

[C] N. Chernov: private communication

[CELS] N. Chernov, G. Eyink, J.E. Lebowitz, Ya.G. Sinai: Steady state electric conductivity in the periodic Lorentz gas, *Commun. in Math. Phys.* **154** (1993), 569–601.

[EM] D.J. Evans, G.P. Morris: *Statistical Mechanics of nonequilibrium fluids*, Accademic Press, San Diego (1990)

[EPR1] J. P. Eckmann, C.-A. Pillet and L. Rey-Bellet: Entropy production in nonlinear, thermally driven Hamiltonian systems. *J. Statist. Phys.* **95** (1999) 305–331.

[EPR2] J. P. Eckmann, C.-A. Pillet and L. Rey-Bellet: Non-equilibrium statistical mechanics of anharmonic chains coupled to two heat baths at different temperatures. *Comm. Math. Phys.* **201** (1999) 657–697.

[ER] J.P. Eckmann, D. Ruelle: Ergodic Theory of Chaos and Strange Attractors, *Rev. Mod. Phys.* **57** (1985) 617–656.

[ES] D. Searles,D.J. Evans: The Fluctuation Theorem and Green-Kubo relations, to appear in JCP

[G] G. Gallavotti: Extension of Onsager's reciprocity relations to large fields and the chaotic hypothesis *Phys. Rev. Lett* **77** (1996) 4334-4337

[GC] G. Gallavotti, E.G.D. Cohen: Dynamical ensamble in stationary states, *J. Stat. Phys.* **80** (1995) 931

[GG] G. Gallavotti, P.L. Garrido: Billiard correlation-functions, *J. Stat. Phys.* **76** (1994) 549-585

[H] W.G. Hoover: *Computational Statistical Mechanics*, Elsevier (1991)

[JLl] M. Jiang, R. de la LLave: Smooth dependence of thermodynamic limits of SRB-measures mp_arc/99-122

[KD] R. Klages, J.R. Dorfman: Simple Maps with Fractal Diffusion Coefficients, *Phys. Rew. Lett.* **74** (1995) 387-390

[LNRM] J. Lloyd, M. Niemeyer, L. Rondoni, G.P. Morris: The non-equilibrium Lorentz gas, *Chaos* **5** (1995) 536-551

[LS] J.L. Lebowitz, H. Spohn: A Gallavotti-Cohen type symmetry in the large deviation functional for Stochastic Dynamics, *J. Stat. Phys.* **95** (1999) 333

[MH] B. Moran, W.G. Hoover: Diffusion in the periodic Lorentz billiard *J. Stat. Phys.* **48**(1987) 709

[NR] W.H. Press, B.P. Flannery, S.A. Teukolsky, W.T. Wetterling *Numerical recipes in C*, Cambridge University Press (1993)

[R] D. Ruelle: Differentiation of SRB states *Commun. Math. Phys.* **187** (1997) 227-241 and Nonequilibrium statistical mechanics near equilibrium: computing higher-order terms *Nonlinearity* **11** (1998) 5-18

[Y] L.-S. Young: Statistical properties of systems with some hyperbolicity including certain billiards, *Annals of Math.* to appear